

See discussions, stats, and author profiles for this publication at: <https://www.researchgate.net/publication/245234943>

# Nitrogen, Sulfur, and Chlorine Transformations during the Pyrolysis of Straw

ARTICLE *in* ENERGY & FUELS · SEPTEMBER 2010

Impact Factor: 2.79 · DOI: 10.1021/ef1007215

---

CITATIONS

28

---

READS

64

6 AUTHORS, INCLUDING:



[Xuebin Wang](#)

Xi'an Jiaotong University

47 PUBLICATIONS 239 CITATIONS

[SEE PROFILE](#)



[Houzhang Tan](#)

Xi'an Jiaotong University

52 PUBLICATIONS 365 CITATIONS

[SEE PROFILE](#)



[M. Pourkashanian](#)

The University of Sheffield

613 PUBLICATIONS 8,200 CITATIONS

[SEE PROFILE](#)

## Nitrogen, Sulfur, and Chlorine Transformations during the Pyrolysis of Straw

Xuebin Wang,<sup>†</sup> Jipeng Si,<sup>†</sup> Houzhang Tan,<sup>\*,†,‡</sup> Lin Ma,<sup>‡</sup> Mohamed. Pourkashanian,<sup>‡</sup> and Tongmo Xu<sup>†</sup>

<sup>†</sup>State Key Laboratory of Multiphase Flow in Power Engineering, Xi'an Jiaotong University, Xi'an 710049, China, and

<sup>‡</sup>Centre for Computational Fluid Dynamics, School of Process, Environmental and Materials Engineering, University of Leeds, LS2 9JT, United Kingdom

Received June 9, 2010. Revised Manuscript Received August 12, 2010

Transformation of nitrogen, sulfur, and chlorine during straw pyrolysis at temperatures from 35 to 1450 °C was investigated by using the coupled thermogravimetry–differential scanning calorimetry–mass spectrometry (TG-DSC-MS) techniques and compared with that of coal. The characteristics of the residual solid char from the straw were analyzed using x-ray diffraction (XRD). Results show that all the nitrogen species (HCN, NH<sub>3</sub>, HNCO, and CH<sub>3</sub>CN), chloric species (HCl and Cl<sub>2</sub>), and sulfur species (SO<sub>2</sub>, H<sub>2</sub>S and COS) began to release from straw from 200 °C, compared with 350 °C for the case of coal. Most of the gaseous species from the straw were released in the form of a sharp peak, compared with the coal which has a much wider peak. NH<sub>3</sub> and HNCO were the primary nitrogen species for both straw and coal; however for the straw the amount of NH<sub>3</sub> released was much higher than that of HNCO. Sulfur species from the straw pyrolysis are sparse, and there was only a little COS released. During coal pyrolysis no COS was detected at all and H<sub>2</sub>S was mainly formed at 500 °C–600 °C. SO<sub>2</sub> was released in three stages (300–500 °C, 500–600 °C and 1200–1450 °C), and the largest SO<sub>2</sub> emission was found at high temperatures due to the decomposition of sulfate. The major chloric species from the pyrolysis of both straw and coal was HCl, and the ion current intensity of Cl<sub>2</sub> was very low. There was a critical temperature of around 800 °C, beyond which most of the chlorine would be released.

### Introduction

Traditional biomass energy accounts for approximately 13% of the global energy consumption, and an estimated 54 GW of biomass power capacity was in place globally by the end of 2009.<sup>1,2</sup> With the aggravation of global greenhouse effect and energy shortage, biomass has more and more been focused as a renewable fuel.

An investigation on the content of nitrogen, sulfur, and chlorine in biomass used in China has been performed in 12 biomass-fired power plants, as shown in Figure 1 and Table 1. Results show that nitrogen content in most biomass can reach 1%; although sulfur content in most biomass is much lower than coal, some can reach up to almost 0.3%. The investigation suggests that the content of N and S in biomass is not always much lower than coal; previous tests on the biomass furnace have shown that the utilization of huge amount of

biomass may still induce the emission of NO<sub>x</sub>,<sup>2–12</sup> and SO<sub>2</sub> from the sulfur in biomass is also considered to play an important role in the corrosion processes.<sup>2,9–11,13,14</sup> Meanwhile, the data also show that the chlorine content in all the biomass except for wood is significantly higher than that in the coal, which also leads to severe problems of corrosion during the utilization of biomass.<sup>2,9,10,13,15,16</sup>

The utilization of biomass for power generation mainly relies on the process of the transformation of thermochemistry, and the process of pyrolysis is one of the most important steps.<sup>17</sup> During the process of biomass pyrolysis, there is still a certain degree of emission of nitrogenous species (NH<sub>3</sub>, HCN, and HNCO),<sup>18–25</sup> chlorine species (Cl<sub>2</sub> and HCl),<sup>16,26,27</sup> and a

\*To whom correspondence should be addressed. E-mail: tanhouzhang@yahoo.cn.

(1) Sawin, J. L.; Martinot, E. In Renewables 2010 Global Status Report. Renewable Energy Policy Network for the 21st Century: 2010; 2010.

(2) Khan, A. A.; de Jong, W.; Jansens, P. J.; Spliethoff, H. *Fuel Process. Technol.* **2009**, *90*, 21–50.

(3) Lin, W.; Jensen, P. A.; Jensen, A. D. *Energy Fuels* **2009**, *23*, 1398–1405.

(4) Mahmoudi, S.; Baeyens, J.; Seville, J. P. K. *Biomass Bioenergy* **2010**, *34*, 1393–1409.

(5) Teixeira, F. N.; Lora, E. S. *Biomass Bioenergy* **2004**, *26*, 571–577.

(6) Salzmann, R.; Nussbaumer, T. *Energy Fuels* **2001**, *15*, 575–582.

(7) Ma, L.; Jones, J. M.; Pourkashanian, M.; Williams, A. *Fuel* **2007**, *86*, 1959–1965.

(8) Nimmo, W.; Daood, S. S.; Gibbs, B. M. *Fuel* **2010**, *89*, 2945–2952.

(9) Obernberger, I. *Biomass Bioenergy* **1998**, *14*, 33–56.

(10) Werther, J.; Ogada, T. *Prog. Energy Combust. Sci.* **1999**, *25*, 55–116.

(11) Koyuncu, T.; Pinar, Y. *Biomass Bioenergy* **2007**, *31*, 73–79.

(12) Youssef, M. A.; Wahid, S. S.; Mohamed, M. A.; Askalany, A. A. *Appl. Energy* **2009**, *86*, 2644–2650.

(13) Obernberger, I.; Brunner, T.; Bärnthaler, G. *Biomass Bioenergy* **2006**, *30*, 973–982.

(14) Obernberger, I. *Fuel Energy Abstr.* **1997**, *38*, 410.

(15) Jensen, P. A.; Stenholm, M.; Hald, P. *Energy Fuels* **1997**, *11*, 1048–1055.

(16) Jensen, P. A.; Frandsen, F. J.; Dam-Johansen, K.; Sander, B. *Energy Fuels* **2000**, *14*, 1280–1285.

(17) Streibel, T.; Geissler, R.; Saraji-Bozorgzad, M.; Sklorz, M.; Kaisersberger, E.; Denner, T.; Zimmermann, R. *J. Therm. Anal. Calorim.* **2009**, *96*, 795–804.

(18) Lepptilahti, J. *Fuel* **1995**, *74*, 1363–1368.

(19) Skreiberg, Ø.; Glarborg, P.; Jensen, A.; Dam-Johansen, K. *Fuel* **1997**, *76*, 671–682.

(20) Li, C.-Z.; Tan, L. L. *Fuel* **2000**, *79*, 1899–1906.

(21) Tan, L. L.; Li, C.-Z. *Fuel* **2000**, *79*, 1883–1889.

(22) Hansson, K.-M.; Samuelsson, J.; Tullin, C.; Åmand, L.-E. *Combust. Flame* **2004**, *137*, 265–277.

(23) Stubenberger, G.; Scharler, R.; Zahirovic, S.; Obernberger, I. *Fuel* **2008**, *87*, 793–806.

(24) Ren, Q.; Zhao, C.; Wu, X.; Liang, C.; Chen, X.; Shen, J.; Tang, G.; Wang, Z. *J. Anal. Appl. Pyrolysis* **2009**, *85*, 447–453.

(25) Di Nola, G.; de Jong, W.; Spliethoff, H. *Fuel Process. Technol.* **2010**, *91*, 103–115.



**Figure 1.** Profile of biomass-fired power plants investigated in China.

**Table 1.** Contents of N, S, and Cl in Fuel Used in Biomass-Fired Power Plants of China

No.	fuel	N <sub>d</sub> (%)	S <sub>d</sub> (%)	Cl <sub>d</sub> (%)
1	HS-wheat straw	0.98	0.07	0.450
2	CT-wheat straw	0.64	0.09	0.639
3	MHK-corn stalk	0.42	0.04	0.426
4	JX-wheat straw	0.74	0.30	1.1
5	JX-corn stalk	0.93	0.15	0.054
6	CF-corn stalk	0.77	0.07	0.573
7	CF-sunflower stalk	0.5	0.1	0.856
8	JY-cotton stalk	0.92	0.11	0.159
9	SY-cotton stalk	0.97	0.16	0.187
10	WK-cotton stalk	0.69	0.08	0.26
11	AVT-cotton stalk	0.80	0.14	0.333
12	BC-cotton stalk	0.63	0.20	0.454
13	JZ-corn stalk	1.06	0.23	0.581
14	JZ-wheat straw	0.71	0.23	1.260
15	JZ-cotton stalk	1.07	0.30	0.235
16	JZ-fruit branch	0.51	0.06	0.021
17	BY-cotton stalk	0.65	0.1	0.264
18	BY-corn stalk	0.79	0.11	0.195
19	BY-fruit branch	0.62	0.06	0.049
20	BY-wheat straw	0.46	0.22	1.051
coal	HT-bituminous coal	0.84	0.58	0.014

spot of sulfur species (COS, SO<sub>2</sub>, and H<sub>2</sub>S).<sup>28–30</sup> In order to control the emissions of NO<sub>x</sub> and SO<sub>2</sub>, and to reduce the corrosion of chlorine during biomass combustion, a better understanding on the conversion of nitrogen, sulfur, and chlorine during biomass pyrolysis is essential and continues to be a challenge.<sup>24,31</sup>

The method of thermogravimetry (TG) analysis has been widely used to investigate the decomposition of biomass during the temperature programmed process, and it could also be coupled with precise analytic equipments such as FTIR, MS, and GC to monitor the emission of gaseous species online and to demonstrate the reaction mechanism of the pyrolyzation.<sup>17,20,25,32–43</sup> However, the special investigation on the

**Table 2.** Ultimate and Proximate Analysis of Straw and Huating-Coal

fuel	proximate analysis (wt %)			ultimate analysis (% wt)					
	M <sub>ad</sub>	A <sub>ad</sub>	V <sub>ad</sub>	C <sub>d</sub>	H <sub>d</sub>	N <sub>d</sub>	O <sub>d</sub>	S <sub>d</sub>	Cl <sub>d</sub>
straw	3.88	6.01	72.10	47.87	4.28	0.99	44.77	0.34	0.237
HT-coal	7.03	18.73	27.89	65.47	3.43	0.84	10.38	0.58	0.014



**Figure 2.** TG-DSC-MS system.

emission of nitrogen, sulfur, and chlorine during biomass pyrolysis using TG is still relatively rare.

In the present paper, the combined TG-DSC-MS techniques are employed to investigate the emission of gaseous species containing nitrogen, sulfur, and chlorine during the process of straw pyrolysis and are compared with coal pyrolysis. The heating process in the TG is simulated in a fixed bed to obtain residual chars at different heating temperature, and the chars are analyzed with XRD to reveal the transformation of the function groups and crystal structures of the residual solid fuel during the process of straw and coal pyrolysis.

## Experimental Setup

**Fuel Properties.** The wheat straw used in this study was from Shannxi province, and the coal is the Huating bituminous (HT-coal) from Gansu province in China. After milling and sieving into 50–200 μm in diameter, the samples were dried in the oven at 105 °C for 24 h. The ultimate and proximate analysis of fuels has been shown in Table 2.

**Experimental Apparatus and Method of TG-DSC-MS.** The TG-DSC-MS system employed consists of Netzsch STA449C thermogravimetry analyzer coupled with Netzsch QMS 403C mass spectrometer, as is shown in Figure 2. To avoid secondary reactions, the probe was very close to the sample crucible, and the gas line between the TG and the MS was heated to 240 °C in order to avoid the condensing of organic species.

- (26) Björkman, E.; Strömberg, B. *Energy Fuels* **1997**, *11*, 1026–1032.  
 (27) Wei, X.; Schnell, U.; Hein, K. R. G. *Fuel* **2005**, *84*, 841–848.  
 (28) Serio, M. A.; Bassilakis, R.; Kroo, E.; Wójtowicz, M. A. *Fuel Chemistry Division Preprints* **2002**, *47*, 588–562.  
 (29) Serio, M. A.; Kroo, E.; Wójtowicz, M. A. *Fuel Chem. Div. Prepr.* **2003**, *48*, 584–589.  
 (30) Ma, S.; Lu, J.; Gao, J. *Energy Fuels* **2002**, *16*, 338–342.  
 (31) Di Blasi, C. *Prog. Energy Combust. Sci.* **2008**, *34*, 47–90.  
 (32) Liu, Q.; Wang, S.; Zheng, Y.; Luo, Z.; Cen, K. *J. Anal. Appl. Pyrolysis* **2008**, *82*, 170–177.  
 (33) Meng, H. H.; Zhang, Q.; Li, X.; Wu, B. *Energy Fuels* **2007**, *21*, 2245–2249.  
 (34) Tao, L.; Zhao, G. B.; Qian, J.; Qin, Y. K. *J. Haz. Mater.* **2010**, *175*, 754–761.  
 (35) Souza, B. S.; Moreira, A. P. D.; Teixeira, A. *J. Therm. Anal. Calorim.* **2009**, *97*, 637–642.

- (36) Giuntoli, J.; Arvelakis, S.; Spliethoff, H.; de Jong, W.; Verkooijen, A. H. M. *Energy Fuels* **2009**, *23*, 5695–5706.  
 (37) Sun, Z.; Jin, B.; Zhang, M.; Liu, R.; Zhang, Y. *Energy* **2008**, *33*, 1224–1232.  
 (38) Bedyk, T.; Nowicki, L.; Stolarek, P.; Ledakowicz, S. *Pol. J. Chem. Technol.* **2008**, *10*, 1–5.  
 (39) Aracil, I.; Font, R.; Conesa, J. A.; Fullana, A. *J. Anal. Appl. Pyrolysis* **2007**, *79*, 327–336.  
 (40) Meszaros, E.; Jakab, E.; Varhegyi, G. *J. Anal. Appl. Pyrolysis* **2007**, *79*, 61–70.  
 (41) Worasuwannarak, N.; Sonobe, T.; Tanthapanichakoon, W. *J. Anal. Appl. Pyrolysis* **2007**, *78*, 265–271.  
 (42) Li, J.; Wang, Z.; Yang, X.; Hu, L.; Liu, Y.; Wang, C. *J. Anal. Appl. Pyrolysis* **2007**, *80*, 247–253.  
 (43) Biagini, E.; Barontini, F.; Tognotti, L. *Ind. Eng. Chem. Res.* **2006**, *45*, 4486–4493.

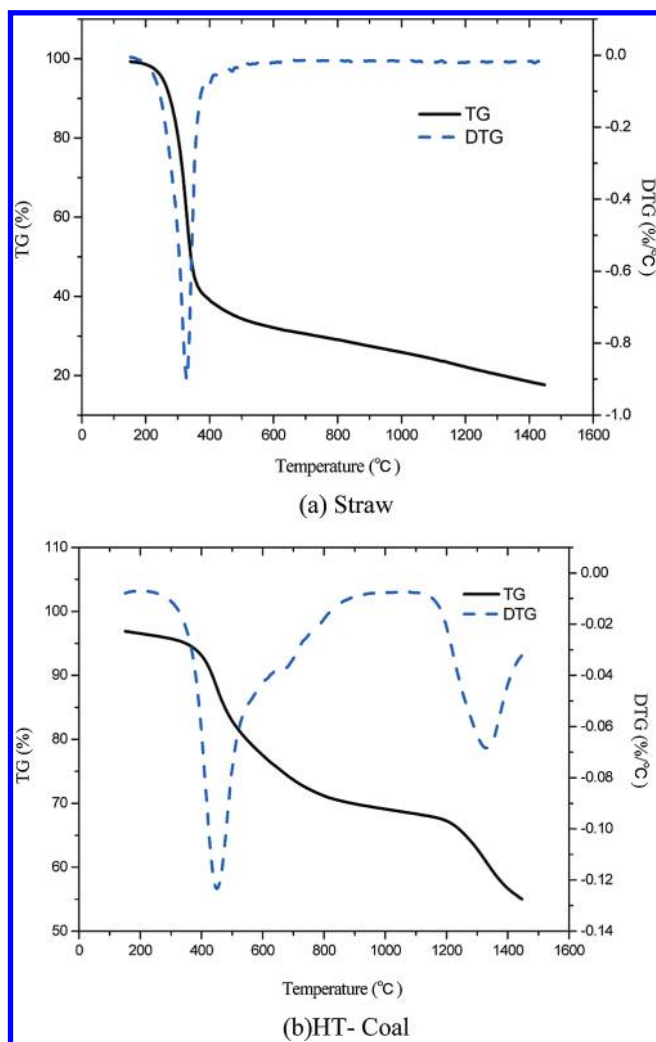


Figure 3. TG-DTG curves for the straw and HT-coal investigated.

In the experiments that have been carried out in this work, approximately 4 mg of straw and 14 mg of HT-coal were used respectively with an argon flow of  $100 \text{ mL} \cdot \text{min}^{-1}$  (> 99.999% purity), linearly heated with a heating rate of  $10 \text{ }^{\circ}\text{C} \cdot \text{Min}^{-1}$  from 35 to 1450  $^{\circ}\text{C}$ .

**Characterization of the Functional Groups in the Residual Char.** To investigate the changes in functional groups and crystal structures during the pyrolysis, X-ray diffraction (XRD) was employed to analyze the residual chars obtained at different heating temperature in the fixed bed. The straw, and coal, samples of 2 g were heated from 35  $^{\circ}\text{C}$  to a target temperature with a heating rate of  $10 \text{ }^{\circ}\text{C} \cdot \text{min}^{-1}$  under inert atmosphere in a quartz reactor of a tube furnace and then quickly cooled to room temperature to be used for XRD analysis. The char from straw was prepared under different target temperatures of 200, 275, 325, 400, 600, and 800  $^{\circ}\text{C}$ ; and the char from HT-coal was prepared under 350, 400, 450, 600, 800, and 1400  $^{\circ}\text{C}$ .

The XRD patterns were obtained from a PANalytical X'pert MPD Pro diffract meter using Ni-filtered Cu-K $\alpha$  irradiation.

## Results and Discussion

**Profile of TG-DTG.** From results of TG and DTG presented in Figure 3, it is shown that there was only one degradation step for straw pyrolysis, Figure 3a, but two steps for coal pyrolysis, Figure 3b. For the pyrolysis of straw shown in Figure 3a, 70% of the mass was lost in the

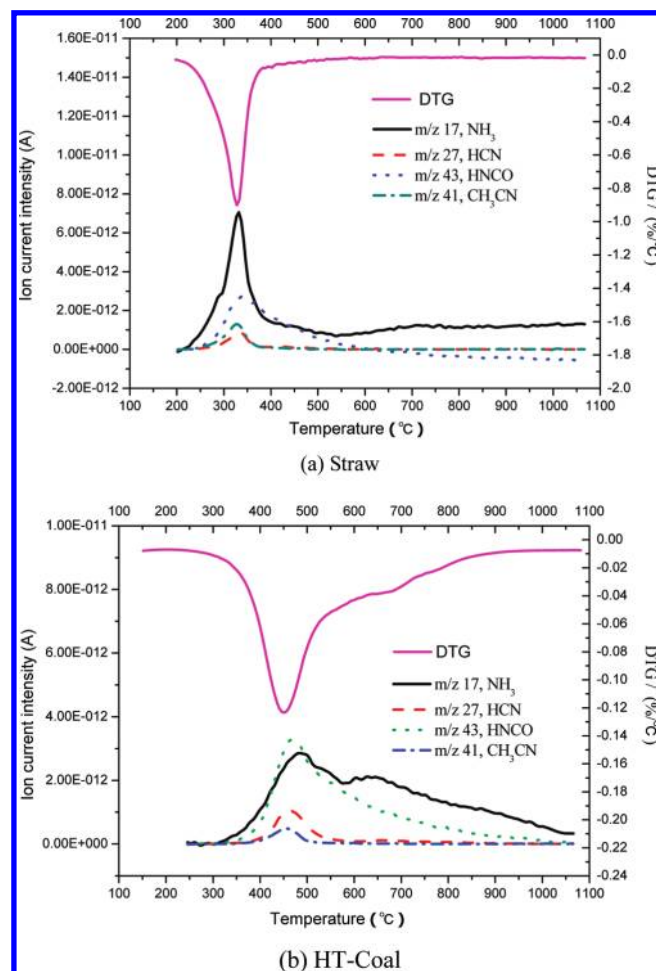


Figure 4. Emission of nitrogen species during the pyrolysis of straw and coal.

temperature range of 200–500  $^{\circ}\text{C}$ , and the maximum rate of weight loss occurred at the temperature of about 325  $^{\circ}\text{C}$ . There was a sharp peak in the DTG profile, indicating that the evolution of volatile was intensive, and it was also in accordance with the previous results of straw pyrolysis by TG-FTIR.<sup>36,44,45</sup> The first stage of the coal pyrolysis, that is, the volatile evolution, started from about 350  $^{\circ}\text{C}$ , see Figure 3b, and ended at about 800  $^{\circ}\text{C}$ , with a peak mass loss at about 450  $^{\circ}\text{C}$ . The second peak of coal pyrolysis took place at a temperature above 1200  $^{\circ}\text{C}$ , which should be lead by the decomposition of sulfate in the coal ash. During the pyrolysis of straw, there was not a second peak, and this is because the ash and the sulfate content of straw were low.

**Emission of Nitrogen Species.** Emission of nitrogen species  $\text{NH}_3$  ( $m/z = 17$ ),  $\text{HCN}$  ( $m/z = 27$ ),  $\text{HNCO}$  ( $m/z = 43$ ), and  $\text{CH}_3\text{CN}$  ( $m/z = 41$ ) during the pyrolysis are shown in Figure 4. It was observed that the nitrogen species started to release at about 250 and 350  $^{\circ}\text{C}$  for straw and coal, respectively, and their peaks of ion current intensity appeared at about 350 and 475  $^{\circ}\text{C}$ , corresponding to the peaks in the DTG curves shown in Figure 3. During the pyrolysis of straw, the ion current intensity of  $\text{NH}_3$  was much higher and sharper than the others;  $\text{HNCO}$  was also a main nitrogenous product; the

(44) Basilakis, R.; Carangelo, R. M.; Wójtowicz, M. A. *Fuel* **2001**, 80, 1765–1786.

(45) Jensen, A.; Dam-Johansen, K.; Wójtowicz, M. A.; Serio, M. A. *Energy Fuels* **1998**, 12, 929–938.



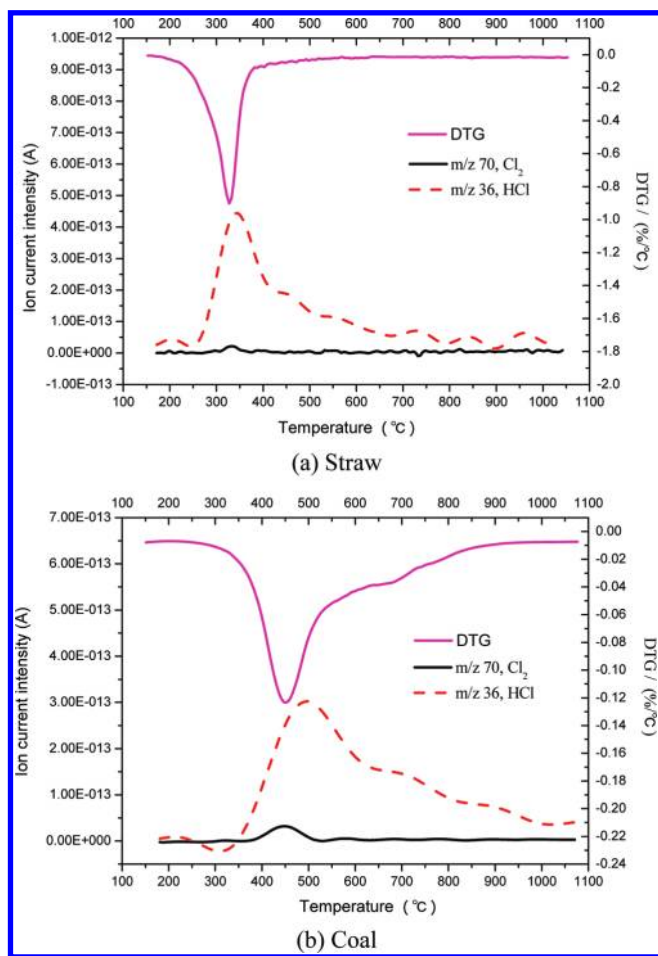


**Figure 5.** Emission of chloric species during the pyrolysis of straw and coal.

profiles of HCN and  $\text{CH}_3\text{CN}$  were almost claps on top of each other, with the intensity of HCN slightly lower than  $\text{CH}_3\text{CN}$ , and this was because the decomposition temperature of straw was low and the function group  $-\text{CN}$  in larger molecules could not be effectively broken to form HCN. By contrast, the ion current intensity of  $\text{NH}_3$  and HNCO for coal pyrolysis was not far off, and the emission peaks, in particular for  $\text{NH}_3$ , were much wider. The intensity of HCN was higher than that of  $\text{CH}_3\text{CN}$ , because the decomposition temperature of coal was much higher, and it was sufficient for the larger molecules containing for the  $-\text{CN}$  to be broken to form more HCN.

It was suggested that the difference between straw and coal pyrolysis should be related to the different nitrogenous functional groups in the fuels: nitrogen was mainly in the form of amino acids and proteins in biomass,<sup>46</sup> and mainly in the forms of heterocyclic nitrogen (pyridine-N and pyrrole-N) in coal.<sup>47,48</sup> Most of the previous researches of biomass decomposition in fixed bed and TG also indicated that  $\text{NH}_3$  is the most substantial nitrogenous product, and the content of  $\text{NH}_3$  is larger than that of HCN and HNCO.<sup>24,46,49</sup>

(46) Becidan, M.; Skreiberg, Ø.; Hustad, J. E. *Energy Fuels* **2007**, *21*, 1173–1180.

(47) Tan, H.; Wang, X.; Wang, C.; Xu, T. *Energy Fuels* **2009**, *23*, 1545–1550.

(48) Kambara, S.; Takarada, T.; Toyoshima, M.; Kato, K. *Fuel* **1995**, *74*, 1247–1253.

(49) Ren, Q.; Zhao, C.; Wu, X.; Liang, C.; Chen, X.; Shen, J.; Wang, Z. *Fuel* **2010**, *89*, 1064–1069.

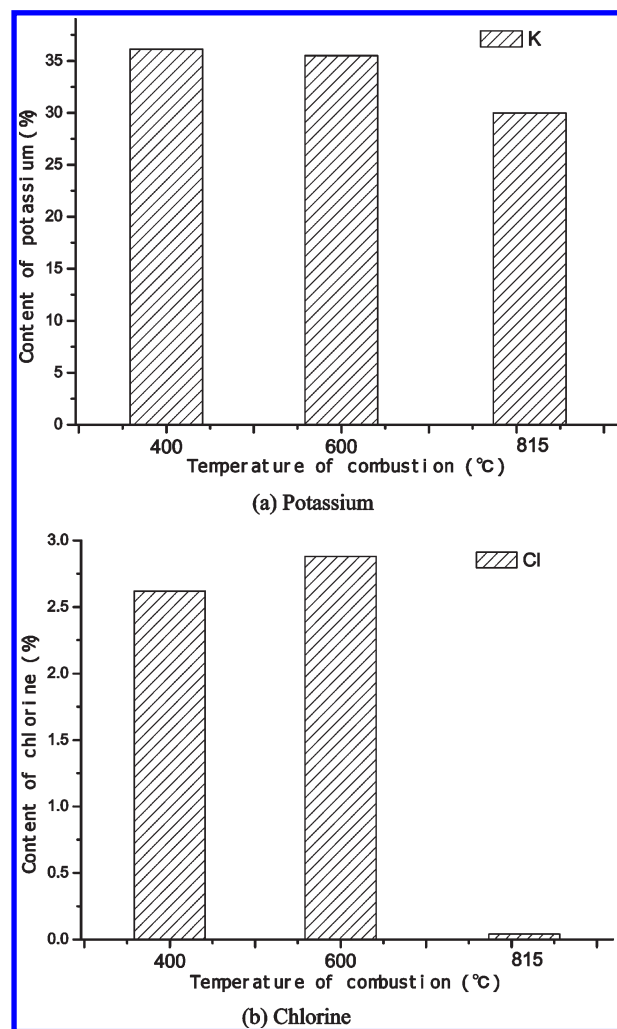


**Figure 6.** Content of potassium and chlorine in ash at different temperatures.

However, the result of Giuntoli<sup>50</sup> has shown that the distribution of nitrogenous products are also related with the biomass type; HNCO is the main nitrogenous specie during the pyrolysis of chicken manure. Meanwhile, further research on the pyrolysis of nitrogen-containing model compounds and biomass residue also demonstrate that the decomposition of protein in biomass undergoes a first stage of deamination to produce  $\text{NH}_3$ , followed by the formation of intermediate compound to produce HCN and HNCO at higher temperature.<sup>22,31,42,50</sup>

**Emission of Chlorine Species.** During the thermal conversion of combustion and gasification of straw, the initial important process is the pyrolysis, at which the chlorine and alkali metals could be released to the flue gas, and it could subsequently cause severe problems of deposition and corrosion.<sup>9,13,15,16</sup> Most of the chlorine is released as HCl and KCl into the flue gas at 800 °C, which are formed both in the devolatilization and in the char combustion phase, and some of it also can condense on small particles of the fly ash.<sup>26</sup>

Figure 5 shows the evolution profile of chloric species HCl ( $m/z = 36$ ) and  $\text{Cl}_2$  ( $m/z = 70$ ). It was indicated that the major chloric product of pyrolysis was HCl for both straw and coal, and the ion current intensity of  $\text{Cl}_2$  was much lower

(50) Giuntoli, J.; de Jong, W.; Arvelakis, S.; Spliethoff, H.; Verkooijen, A. H. M. *J. Anal. Appl. Pyrolysis* **2009**, *85*, 301–312.

**Table 3. Mass and Content of K and Cl in the Residual Ash at Different Temperatures**

temperature (°C)	mass of ash (g)	content of K (%)	content of Cl (%)	mass of K (g)	mass of Cl (g)
400	0.0762	36.13	2.62	0.0275	0.0020
600	0.0701	35.49	2.88	0.0249	0.0020
815	0.0601	29.99	0.04	0.0180	0.0000

than that of HCl, and in particular, the signal of Cl<sub>2</sub> for straw pyrolysis was very weak, existing only in the temperature range of 300–350 °C for straw and 400–500 °C for coal. After the first peak in the DTG curve, there was no additional Cl<sub>2</sub> release.

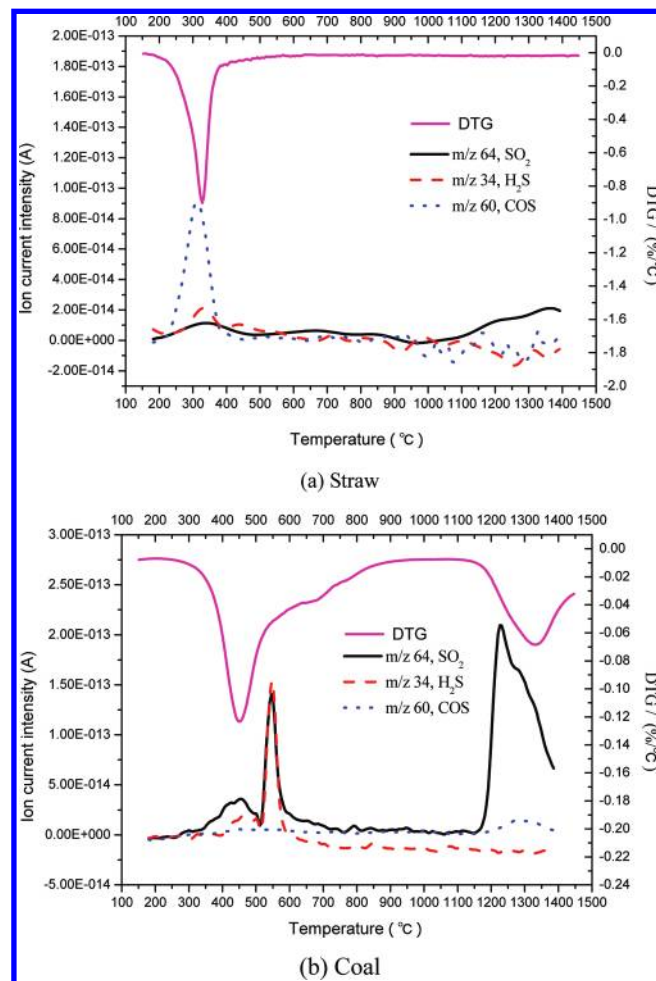
However, it should be noted that, the ion current intensity curve of HCl for straw pyrolysis was much wider than the DTG curve shown in Figure 3a and nitrogen species emission curve shown in Figure 4a; therefore, it suggests that with the increase in the temperature, chlorine was still released continuously after the end of the major volatile release until the temperature reached to about 800 °C. The continuous emission of chlorine was a result of the volatility of chloride in the ash of the straw.

To further verify the transformation of chlorine in ash, 1 g of straw was burned in a muffle furnace for 2.5 h to prepare the ash sample at different temperatures, that is, 400, 600, and 815 °C, and the ash samples were analyzed by X-ray fluorescence (XRF) to analyze the content of chlorine and potassium. Results are shown in Figure 6, and they indicate that with the temperature increasing from 400 to 600 °C, the content of potassium in the ash decreased, mainly from the metals associated with the organic phase.<sup>51,52</sup> However, the content of chlorine even increased somewhat with increasing temperature in this scale, which was mainly due to the dilute effect from the continued volatilization of residual organics in ash. The mass of residual ash, potassium, and chlorine have been also listed in Table 3, from which it could be seen that when temperature increased from 400 to 600 °C the mass of potassium decreased by 10%, but there is no change for the mass of chlorine.

When the temperature was increased to 815 °C, Figure 6 and Table 3 show that the content of potassium decreased further and that the mass of potassium also decreased by 30% compared with that at 600 °C. Meanwhile, almost no chlorine remained in the residue ash. Comparing the mass loss of potassium and chlorine in Table 3, it could be found that the mass loss of chlorine was much lower than that of potassium, which indicated that potassium could vaporize as other potassium-containing species besides KCl.<sup>51</sup>

The results from both the pyrolysis in the TG and the combustion in the muffle furnace show a critical limit temperature of around 800 °C for chlorine to be able to remain in the biomass.

**Emission of Sulfur Species.** Emission of sulfur species during straw and coal pyrolysis is shown in Figure 7. Because the content of sulfur in biomass was much lower than that in coal, the ion current intensity of sulfur species from straw pyrolysis was very low, and only COS ( $m/z = 60$ ) was detected in the temperature range of 200–400 °C. Signals of H<sub>2</sub>S ( $m/z = 34$ ) and SO<sub>2</sub> ( $m/z = 64$ ) were extremely weak across the temperature region tested. At temperatures higher than 950 °C, the ion current intensity of SO<sub>2</sub> gradually increased. The distribution of COS and SO<sub>2</sub> is consistent

**Figure 7.** Emission of sulfur species during the pyrolysis of straw and coal.

with the results of Serio<sup>28,29</sup> and Bassilakis,<sup>44</sup> during whose experiment, detected by TG-FTIR, the yield of COS was also higher than SO<sub>2</sub>. It was well known that sulfur in straw mainly existed in two forms: organically bound and inorganic sulfate. It was suggested that at temperatures lower than 400 °C the emission of sulfur species COS and H<sub>2</sub>S were mainly due to the decomposition of organically bound sulfur with a lower stability; the increase of SO<sub>2</sub> at temperatures higher than 950 °C should be from the evaporation or transformation of inorganic sulfate.<sup>53,54</sup>

In contrast, during the process of coal pyrolysis, there was no COS detected, but the intensity of H<sub>2</sub>S and SO<sub>2</sub> signals were much stronger with a single peak for H<sub>2</sub>S at 500–600 °C and three peaks of different levels for SO<sub>2</sub> at 300–500, 500–600, and 1150–1450 °C, respectively. H<sub>2</sub>S was mainly formed in 500–600 °C. At temperatures from 300–600 °C,

(51) Jones, J. M.; Darvell, L. I.; Bridgeman, T. G.; Pourkashanian, M.; Williams, A. *Proc. Combust. Inst.* **2007**, *31*, 1955–1963.

(52) Gjernes, E.; Hansen, L. K. *Energy Fuels* **1996**, *10*, 649–651.

(53) Khalil, R. A.; Seljeskog, M.; Hustad, J. E. *Energy Fuels* **2008**, *22*, 2789–2795.

(54) Knudsen, J. N.; Jensen, P. A.; Dam-Johansen, K. *Energy Fuels* **2004**, *18*, 1385–1399.

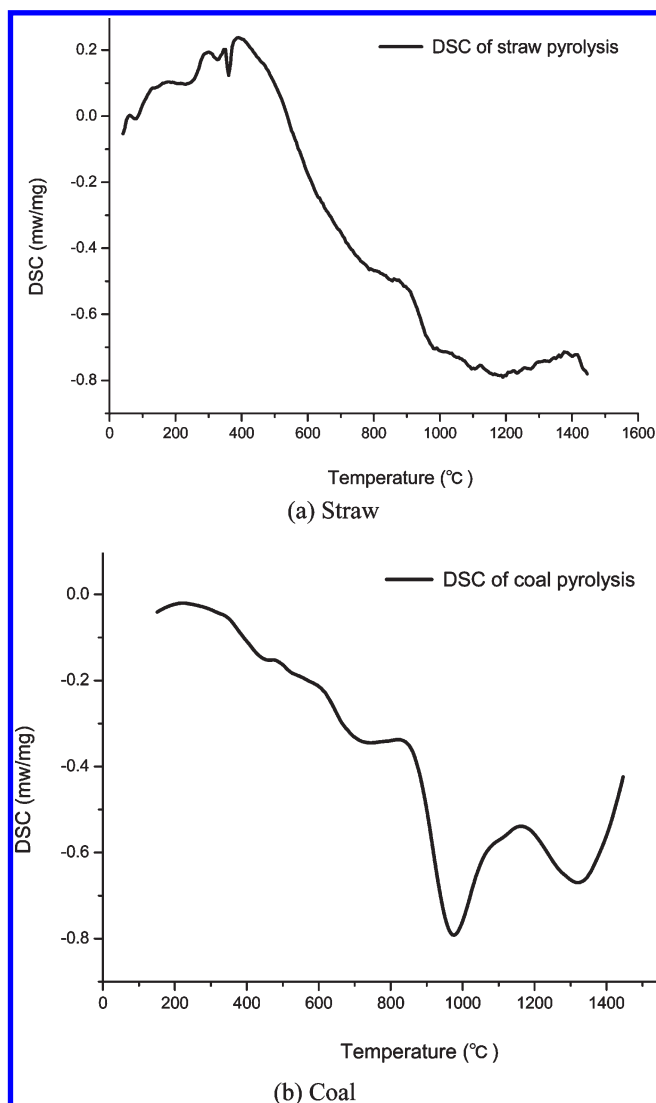


Figure 8. DSC curves during the pyrolysis of straw and coal.

the coal was in the stage of volatile evolution, thus the signal intensity was relatively weak; at 1150~1450 °C the pyrolysis was in the stage of ash decomposition corresponding to the second peak in the DTG curves shown in Figure 2b. It is suggested that the first and second peaks were due to the break of functional group of organic sulfur in the volatile, and the last peak was due to the decomposition of sulfate in coal ash.<sup>55,56</sup>

**Detection of DSC Curve.** The DSC profiles for straw and coal pyrolysis were shown in Figure 8, and they confirmed that the two processes were endothermic. There was not a clear endothermic characteristic peak in the DSC curve for straw; however, a large characteristic peak appeared in the range of 1150~1450 °C for coal, corresponding to the peaks shown in Figures 3b and 7b in this temperature range. Furthermore, it indicated that the second peaks in the DTG and DSC curves of coal pyrolysis should be due to the decomposition of sulfate in coal ash.

**Characteristics of Residual Char.** To investigate the transformation of residual solid char and provide supporting information of emission of gaseous species, XRD analysis

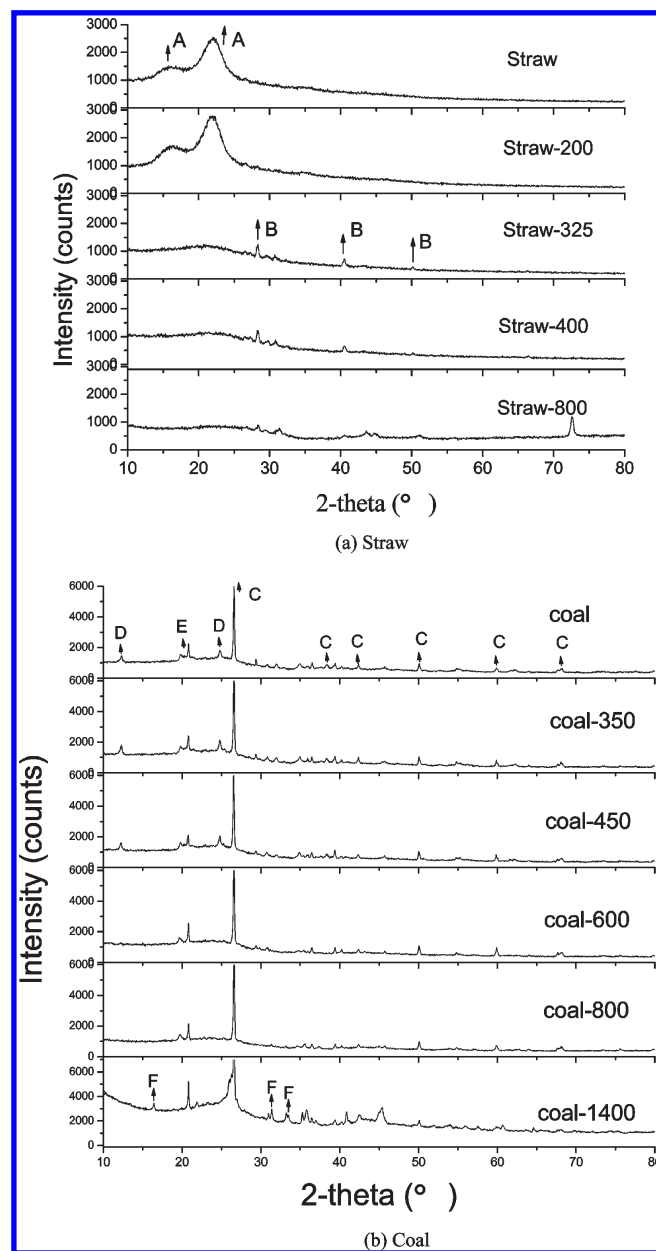


Figure 9. XRD spectra for straw char and coal char prepared at different temperatures (A:  $C_5H_{12}O_5$ ; B: KCl; C:  $SiO_2$ ; D:  $Al_2SiO_5(OH)_4$ ; E:  $Na_2S_2O_3$ ; F:  $Al_2(Al_{2.8}Si_{1.2})O_{9.54}$ ).

was performed on coal and biomass char, and the results are shown in Figure 9.

By comparing the XRD spectra of original straw and coal before pyrolysis, it was noted that the peaks of crystal structure in coal were much sharper than that in straw. There were two wide peaks for organic functional group xylitol at 15 and 25°; however, no organic functional group peak was observed for coal. Instead, it has a large number of sharp peaks of inorganic crystal components.

Figure 9a showed that when the decomposition temperature increased to above 325 °C, the wide peaks of xylitol ( $C_5H_{12}O_5$ ) in straw have disappeared, indicating that large organic molecules decomposed at this temperature. After the disappearance of the wide peaks, the crystal peaks of KCl were revealed, and this indicated that the peaks of KCl should be shadowed by the wider and bigger peak of the xylitol groups. However, when the temperature increased

(55) Attar, A. *Fuel* 1978, 57, 201–212.

(56) Liu, C. L.; Hackley, K. C.; Coleman, D. D. *Fuel* 1987, 66, 683–687.

beyond 800 °C, the characteristic peak of KCl became very weak. This indicated that KCl might have volatilized from the residual char at about 800 °C, and it was corresponding to the results in Figures 5a and 6. The critical temperature 800 °C was in accord with the results of experiment and dynamic modeling by Wei.<sup>27,57</sup>

Figure 9b showed that at temperatures lower than 800 °C, the XRD spectra of coal char remained almost unchanged, and the major crystal peaks were quartz, kaolinite, and sodium sulfate. When the decomposition temperature increased to 1400 °C, the characteristic peaks of sodium sulfate were weakened significantly, and the new characteristic peaks of mullite were formed. This also indicated the decomposition of sulfate and the formation of aluminum silicate, and this was in consistence with the observations on the last peak of DTG in Figure 3b, the last peak of SO<sub>2</sub> emission in Figure 7b, and the second endothermic peak of DSC in Figure 8b.

### Conclusion

In this paper, the transformation of nitrogen, sulfur, and chlorine during the process of straw pyrolysis was investigated by a combined TG-DSC-MS technique and compared with that of coal. The functional groups and crystal structures in the residual chars at different temperatures were examined by XRD. The main conclusions are summarized as follows:

(1) NH<sub>3</sub> and HNCO were the primary nitrogen species for both straw and coal. For the pyrolysis of straw, NH<sub>3</sub> was

produced at a lower temperature than HNCO, and the content of NH<sub>3</sub> was much higher than that for coal pyrolysis, which was related to the different nitrogenous functional groups existing in the straw and coal.

(2) COS was the major sulfur species during the pyrolysis of straw. The release of COS and H<sub>2</sub>S from the decomposition of organic sulfur finished at a lower temperature than 400 °C; meanwhile, the content of SO<sub>2</sub> increased obviously at higher temperatures than 950 °C, which was from the transformation of inorganic sulfate. During coal pyrolysis no COS release was detected, and H<sub>2</sub>S was mainly formed in the range 500–600 °C. SO<sub>2</sub> was released from coal pyrolysis in three stages (300–500, 500–600, and 1200–1450 °C). Both DSC and XRD data indicated that the largest SO<sub>2</sub> emission at high temperatures was due to the decomposition of sulfate.

(3) The major chloric species from the pyrolysis of both straw and coal was HCl. The content of Cl<sub>2</sub> was much lower, and Cl<sub>2</sub> was mainly formed in the temperature range of 300–350 °C for straw pyrolysis and 400–500 °C for coal pyrolysis. Analysis on the biomass ash and char at different temperatures also suggested that mass loss of chlorine was much lower than that of potassium, which indicated that potassium vaporized as other potassium-containing species besides KCl. All the results of TG-DSC-MS, XRF, and XRD show that there was a critical temperature of around 800 °C, beyond which most of the chlorine would be released.

(57) Wei, X.; Lopez, C.; von Puttkamer, T.; Schnell, U.; Unterberger, S.; Hein, K. R. G. *Energy Fuels* 2002, 16, 1095–1108.

**Acknowledgment.** The present work was supported by the Natural Science Funds of China (No. 50976086).